Oblique Collision in the Northern Zagros Observed by GPS

A. Walpersdorf[1], H.R. Nankali[2], F. Tavakoli[2], M. Tatar[3], D. Hatzfeld[1], P. Vernant[4], and J. Chéry[4]

1. Laboratoire de Géophysique Interne et Tectonophysique, Maison des Géosciences, BP 53, 38041 Grenoble Cedex 9, France, email: walpersdorf@obs.ujf-grenoble.fr
2. National Cartographic Center, Tehran, I.R. Iran
3. International Institute of Earthquake Engineering and Seismology (IIEES), Tehran, I.R. Iran
4. Laboratoire de Dynamique de la Litosphère, Montpellier, France

ABSTRACT: *The total Arabia-Eurasia collision with 22mm/yr of shortening is absorbed on the Iranian territory mainly in two mountain belts, the Zagros and the Alborz, and on a few large strike-slip faults. Our study focuses on the northern part of the Zagros (west of the NS trending Kazerun fault system), that has been covered by an 18 site GPS network measured in 2001 and 2003. In northern Zagros, shortening is oblique to the mountain belt and partitioning of the deformation on strike-slip and thrust faults could be expected. An example is the pure strike-slip earthquake of magnitude 7.4 on the Main Recent Fault, the major strike-slip fault in northern Zagros, close to Dorud in 1909. Our precise velocities of bedrock sites with forced antenna centring show that 3-6 mm/yr of shortening is occurring in northern Zagros perpendicular to the mountain belt axis, with a total dextral strike-slip component of 4-6mm/yr. A part of this strike-slip motion is found on the Main Recent Fault. The detailed GPS velocity field indicates that the deformation is not completely distributed but can be attributed to some individual faults. However, there is no clear evidence of partitioning. This result will be compared with GPS studies of the central Zagros, where the major deformation mechanism is axis perpendicular shortening with 8mm/yr.*

Keywords: Global Positioning System (GPS); Satellite geodesy; Continental deformation; Plate convergence; Fault motion; Zagros

1. Introduction

The Arabia-Eurasia collision with 3*cm/yr* according to *NUVEL1-A* [2] takes place entirely inside the Iranian borders, see Figure (1). The shortening is concentrated mainly on two mountain ranges, the Alborz in the north and the Zagros in the south. The global present day displacement field is illustrated by the red arrows in Figure (1), a velocity field obtained by two measurement campaigns on the Iran global *GPS* network published by Vernant et al [9]. Their study shows that the actual Arabia-Eurasia shortening takes place with about 22*mm/yr* oriented 7°*N* with respect to stable Eurasia, distributed over the two mountain belts bordering a relatively stable Central Iranian block. No shortening is observed in the Persian Gulf. These *GPS* data are included in the present work. The upward pointing triangles indicate the emplacement of the North Zagros *GPS* network which is the object of the present study, and the downward pointing triangles show the Central Zagros network, which will be presented here for comparison.

A well adapted reference frame for examining the North Zagros kinematics is established by minimizing the velocities on the Central Iranian block. This block is defined here according to Vernant et al [9], and comprises the Iran global sites *MIAN*, *BIJA*, *SHAH*, *ARDA*, *HARA* and *KERM*. The residual velocities with respect to this block are presented in

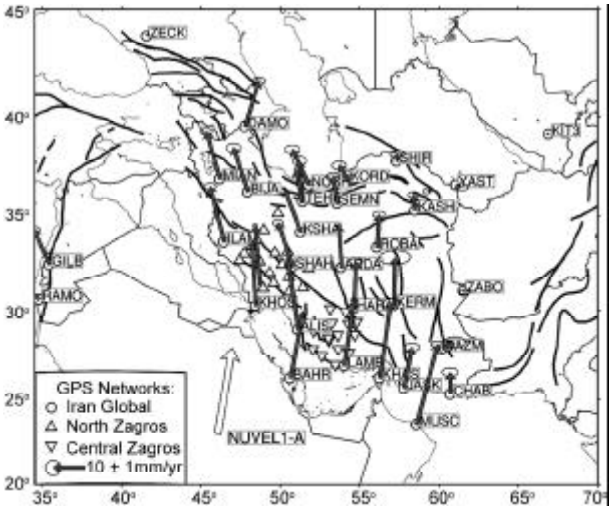

Figure 1. Iranian tectonic settings with the NUVEL1-A predicted shortening rate of 3cm/yr (white vector) and the velocity field on the Iran global GPS network (grey vectors) from [9] with respect to Eurasia. The GPS measurements indicate 22mm/yr of shortening. Upward pointing triangles represent the emplacement of North Zagros GPS stations, downward pointing triangles the Central Zagros network.

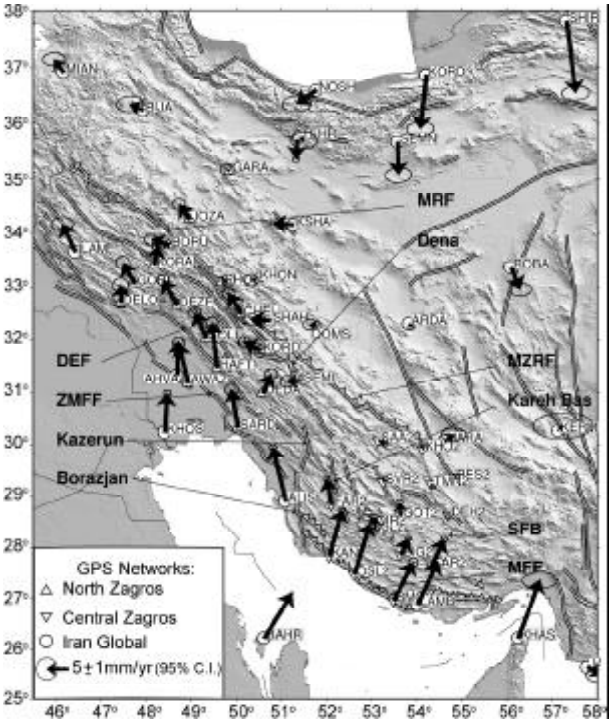

Figure 2. North Zagros and Central Zagros velocity fields with respect to the Central Iranian block. The scale vector corresponds to 5mm/yr. The error ellipses indicate formal errors within a 95% confidence interval. The differential velocities throughout the network give some indications of faults which can be suspected to be active and which are pointed out on the graph with black arrows. DEF: Dezful Embayment Fault; ZMFF: Zagros Mountain Front Fault; MRF: Main Recent Fault; MZRF: Main Zagros Reverse Fault; SFB: Simple Fold Belt; MFF: Main Front Fault [1].

Figure (2). We notice about 8*mm/yr* of shortening between the Persian Gulf coastline and Central Iran.

A model for the present day deformation of the Zagros mountain belt has been proposed in a seismotectonic study by Talebian and Jackson [7]. The authors compile the directions of earthquake slip vectors related to thrust and strike-slip events with respect to the overall constraints given by the NUVEL1-A [2] or REVEL [5] plate models. They conclude that there is a transition from pure shortening in Central Zagros to oblique shortening in North Zagros with some indications for the spatial separation of strike-slip and thrust mechanisms and thus partitioning of the deformation. The transition is accommodated by extension and block rotation. The Kazerun fault system seems to play an important role in the overall deformation mechanism.

The aim of our *GPS* study is to answer the following questions:

- Is the North Zagros deformation field distributed or localized on individual faults?
- Is there any evidence for strain partitioning?
- What is the relation between the North Zagros and the Central Zagros deformation mechanism?

2. GPS Data

The North Zagros *GPS* data presented in this work have been obtained by two measurement campaigns in 2001 and 2003. The North Zagros network consists of 18 bedrock sites with forced antenna centring. The *GPS* sites were occupied with Trimble *SSE* and Ashtech *Z*12 receivers. All *GPS* stations were equipped with choke-ring antenna. The network was completed with 2 Iran Global sites and data from 3 Iranian permanent stations. Each site was observed for at least 48 hours.

For comparison, the data from the Central Zagros network was also presented, a network of 15 sites with conventional markers implying antenna tripod setup. This network has been measured in 1997, 2000 and 2003, the first two epochs being published by Tatar et al [8]. In the last campaign, 3 Iran Global sites have been included, and the 3 permanent Iranian stations have been used in the analyses as soon as available.

The data analysis has been performed with the *GAMIT/GLOBK* 10.1 software [3]. 32 *IGS* stations have been included to establish the reference frame. Final *IGS* orbits have been adjusted in the analysis and corresponding Earth orientation parameters have been used. In the combination of daily solutions with

the Kalman filter (*GLOBK* software), *SOPAC*'s global solution files have been included continuously from December 1997 to November 2003, covering all measurement epoch presented here.

The precision of the inferred site velocities has been evaluated by 1) the campaign repeatabilities, giving the short term scatter of the baseline components; 2) velocity residuals on local rigid tectonic blocks, evaluating long term uncertainties for the campaign stations.

The campaign repeatabilities are given in Table (1). They correspond to the increasing quality of the Central Zagros measurements (longer observation spans and more simultaneous observations by higher number of field teams). For the Central Zagros network, with a mean repeatability of 4 and 1*mm* in 1997 and 2003 respectively on the horizontal components, we could expect velocity uncertainties of 1*mm/yr* over the 6 years observation time span. Mean horizontal repeatabilities of 2*mm* in the 2001 and 2003 North Zagros network yield a 2*mm/yr* precision over the 2 years time span. However, systematic errors like tripod setup (in the Central Zagros network) or antenna phase centre offsets cannot be identified by the repeatability results.

Table 1. Mean repeatabilities on the north, east and up baseline components in each of the 5 campaigns presented in this paper. This statistic is limited on the local North Zagros and Central Zagros network stations with maximum baseline lengths of 3000km.

Campaign	# Baselines	North [mm]	East [mm]	Up [mm]
Central Zagros 1997	25	2.8	3.0	7.4
Central Zagros 2000	144	1.7	2.0	5.2
North Zagros 2001	233	1.1	1.7	4.7
North Zagros 2003	231	0.7	1.5	3.2
Central Zagros 2003	206	0.9	1.3	2.8

Nevertheless, these systematic errors do show up in the comparison of velocities of sites on the same rigid tectonical unit. Two micro-blocks of different size represented by several *GPS* sites can be used in this study to estimate velocity uncertainties: The larger one is the Central Iran block (stations *MIAN, BIJA, SHAH, ARDA, HARA, KERM*, and stations in the northern part of Central Zagros), the smaller one the Persian Gulf plain in the south of North Zagros (stations *KHON, AWAZ, AHVA, SARD, HAFT*). Horizontal residual velocities on the Central Iranian block as defined by Vernant et al [9], of 1.9*mm/yr* were noticed. When 6 Central Zagros stations with low residual velocities with respect to Central Iran (*SAA*2, *KHO*2, *BES*2, *SVR*2, *DEH*2, *TMN*2) were included, the average residuals with respect to rigid motion of this block are evaluated to 1.2*mm/yr*. In the North Zagros Persian Gulf plain, the average residuals of the 5 site velocities are 2.2*mm/yr*. These residuals with respect to rigid block motion evaluate the uncertainty of the velocity estimates presented in this study to ~2*mm/yr* with slightly better values for the Central Zagros measurements due to the 6 years observation span, in spite of the tripod setup in this network.

3. North Zagros Velocity Field and Strain Distribution

The velocity field obtained on the North Zagros network is shown in Figure (2). The reference frame is the Central Iranian block. In the Persian Gulf plain, incoming velocities of 6 to 8*mm/yr* are observed representing the northern part of the Arabian plate. Velocities decrease when entering the Zagros mountain belt. They stabilize at values around 3*mm/yr* in the center of the mountain belt and fade on the northern side of the Main Recent Fault (*MRF*) on the Central Iranian block. This velocity field indicates some significant relative displacement rates which could be related to individual faults: the *MRF* and the Main Zagros Reverse Fault (*MZRF*), the Dena fault as the southeastern continuation of *MRF*, the *NS* trending Kazerun and Borazjan fault system, and the Dezful Embayment Fault (*DEF*) and the Zagros Mountain Front Fault (*ZMFF*) along the boundary between North Zagros and the Persian Gulf plain.

The velocity field has been established with only 2 measurements over a 2 year time span. It seems this is still too early to analyse couples of site velocities to quantify the displacement rate of individual faults. However, the analysis of strain calculated over the whole velocity field or a subset of stations can be used to average the individual velocity observations and obtain a more significant quantification of the deformation in the North Zagros network. The strain tensor obtained over 19 stations in the North Zagros is shown in Figure (3a). Over the whole North Zagros network, a dominating compressive component evaluated to -15.4*nanostrain/yr* and oriented perpendicular to the mountain axis was observed. A weaker extensive component related to a strike-slip component is presented in the overall deformation pattern.

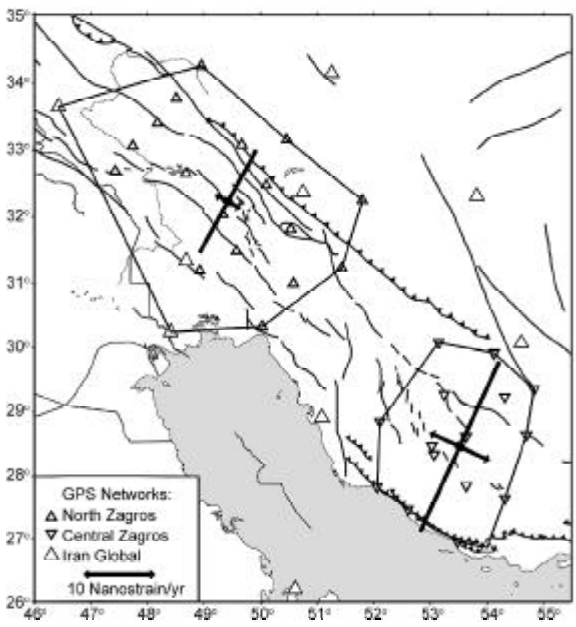

Figure 3a. Overall strain rates in the North and Central Zagros networks. Numerical values are indicated in Table (2).

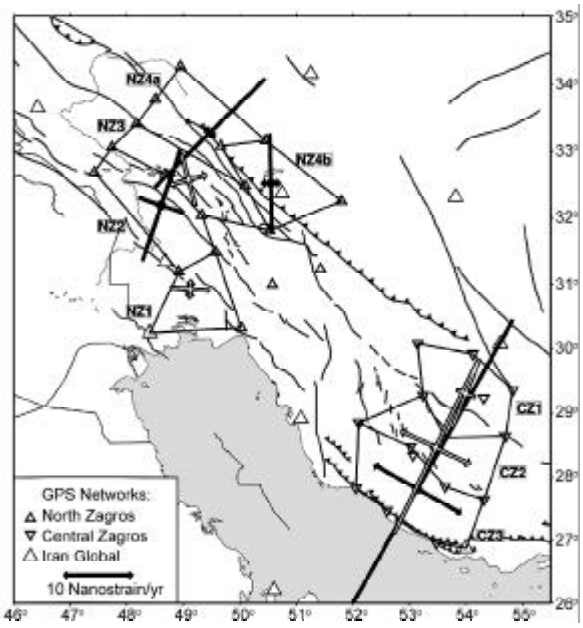

Figure 3b. Strain rates in subnetworks. Black and white strain crosses distinguish relatively high and low deformation rates, respectively.

In Figure (3b), we show the strain distribution in several subnetworks. In the subnetwork *NZ*1 in the Persian Gulf plain in the south which is supposed to be only weakly deformed, strain rates of less than 10*nanostrain/yr* are observed. The next subnetwork *NZ*2 covering the *DEF* reaches a significantly higher strain rate of -16*nanostrain/yr*. Then, the subnetwork NZ3 in the weakly deformed central part of North Zagros shows again low strain rates below 10 nanostrain/yr. Finally, in subnetworks covering the *MRF* and the *MZRF* (*NZ*4*a* and *NZ*4*b*), significant compressive strain rates are shown with -19 and -13*nanostrain/yr*. The numerical values are summarized in Table (2).

The strain rates in subnetworks show that the deformation is not homogeneously distributed but concentrated in zones related to more active faults with respect to others.

4. Comparison North Zagros-Central Zagros Deformation Mechanisms

The velocity field obtained by the combination of the measurements in North and Central Zagros is presented in Figure (2). One dominating feature is that a large northern part of the Central Zagros network is obviously part of the Central Iranian block as demonstrated by the low residual velocities. This means that the *MZRF* is inactive in this part of the Zagros. The major part of the deformation in Central Zagros is concentrated in the southern part of the network.

Comparing the overall strain of North Zagros and Central Zagros, see Figure (3a) and Table (2), we notice higher strain rates on both the compressive and the extensive component in Central Zagros. The decrease of the overall deformation rates from

Table 2. Strain rate values in nanostrain/yr for the main networks, for the 5 North Zagros subnetworks and the 3 Central Zagros subnetworks. The most significant values in the subnetworks are highlighted. For the localization of the subnet works refer to Figure (3b).

	North Zagros	Major Axis	Sec. Axis	Central Zagros	Major Axis	Sec. Axis
Main Networks:	NZ	-16.5 ± 3.0	3.9 ± 2.5	CZ	-27.3 ± 3.0	9.2 ± 2.9
Subnetworks:	NZ1	-5.5 ± 10.8	2.6 ± 9.9	CZ1	-10.7 ± 6.8	-2.6 ± 5.2
	NZ2	**-16.9 ± 14.9**	**-6.8 ± 9.3**	CZ2	-23.4 ± 1.2	11.1 ± 3.8
	NZ3	-7.7 ± 15.1	5.4 ± 15.8	**CZ3**	**-57.0 ± 7.4**	**14.6 ± 3.7**
	NZ4a	**22.5 ± 14.3**	**-2.0 ± 7.8**			
	NZ4b	**-14.2 ± 13.0**	**2.6 ± 11.2**			

Central to North Zagros could be due to two reasons: first, the North Zagros network is a little more extensive than the Central Zagros network, so that the velocity differences are spread over larger distances leading to lower strain; second, the relative motion between Arabia and Eurasia constraining the Zagros deformation decreases from east to west according to their rigid block motion with respect to an Euler pole situated at $27.8 \pm 0.5\ °N$, $18.6 \pm 1.4°E$ with a rotational velocity of $0.40 \pm 0.1°/Ma$ [9]. In Figure (3b), we present strain rates in 3 subnetworks of Central Zagros compared to the North Zagros subnetworks. A quite distinct strain distribution in Central Zagros with respect to North Zagros is observed. The subnetwork *CZ*1 in the stable northern part yields the lowest strain rates of all of the subnetworks with -10 and -3*nanostrain/yr*. Already the intermediate subnetwork *CZ*2 reaches higher strain rates than in any subnetwork in North Zagros. In the southern most subnetwork *CZ*3, the compression rate is evaluated to a maximum value of -57*nanostrain/yr*. The three compressional axes are parallel to each other and perpendicular to the mountain axis represented by the *MZRF*.

In Table (2), those subnetworks are highlighted where most of the deformation occurs: For North Zagros the subnetworks *NZ*2, *NZ*4*a* and *NZ*4*b*, for Central Zagros the subnetwork *CZ*3. The study of strain distribution in North and Central Zagros leads to the following result: We identify as regions of major strain one zone in the south of Central Zagros along the Persian Gulf coast. This zone of major strain is transferred at the localization of the Kazerun fault system to two zones of major deformation in North Zagros. These two zones of major strain are centred on the *DEF* and the *MRF/MZRF*. The Kazerun fault system seems to play an important role in the transfer of strain from Central Zagros to North Zagros.

5. Evolution of the Deformation Mechanism from Central Zagros to North Zagros on Transects Across the Zagros Mountain Axis

Another way to study how the deformation mechanism is evolving from Central Zagros to North Zagros is to look at the velocity distributions on transects across the Zagros mountain belt from south to north. We distribute the site velocities on 5 transects (*TN*1, *TN*2, *TN*3 in the North Zagros, *TC*1 and *TC*2 in Central Zagros) perpendicular to the mountain axis. The mountain axis has been identified schematically by the approximate emplacement of the *MRF*/*MZRF*. The velocity vectors of the closest stations to each of the transects have been projected on the two directions parallel and perpendicular to the mountain axis. These two components will be interpreted as strike-slip and shortening components of the site displacements with respect to the Zagros mountain axis. The two velocity components are displayed on Figure (4) with respect to the distance between the *GPS* site and the approximate emplacement of the *MRF*. This graphical representation shows how the strike-slip and shortening rate evolve with the distance from the major fault, and this on successive transects covering the Zagros from the north to the central part.

On Figure (4), the *MRF/MZRF* emplacement is indicated with the vertical line at 0*km* in each of the graphs. To the right of *MRF/MZRF* is the Central Iranian block with fading velocities.

To analyse the velocity distributions, simple deformation models are superposed to the velocity observations (dark grey lines). For the strike-slip component in the left part of Figure (4), the model describes a locked strike-slip fault in an elastic half space [4].

The numerical values for the total velocities are indicated in the upper part of the graphs. The two curves correspond to two locking depths of 10 and 20 km, showing that this model parameter is not significant for describing the velocity distribution on the spatial scale of the transects. The models are centred on the *MRF*, which is certainly not realistic in some cases (on the Central Zagros transects) or only an incomplete description of the observations in other cases (the North Zagros transects). In the Central Zagros, the velocity field, Figure (2), already showed that deformation is located further south of *MZRF*. In the North Zagros, a part of the deformation can be attributed to the *MRF*, but there seems to be another part localized further south. The total strike-slip velocities vary from 2*mm/yr* in Central Zagros to 4-6*mm/yr* in North Zagros.

The model chosen for the compressive component is simply constant strain over the whole transects in North Zagros, and over the deforming part of the transects in Central Zagros, excluding stations in the stable northern part of the network. This corresponds to a linear velocity distribution. We see increasing strain from North Zagros to Central Zagros. Also, the velocity amplitudes indicate clearly the highest values in Central Zagros (up to 8*mm/yr* with respect to the

Central Iranian block fixed), and decreasing values towards North Zagros (down to 2*mm/yr*).

The comparison of the observed velocities with the models helps identifying discontinuities in the evolution of the site velocities over the distance which can be correlated with the emplacements of some individual faults (indicated by vertical green lines in Figure (4)). In the shortening component (right part

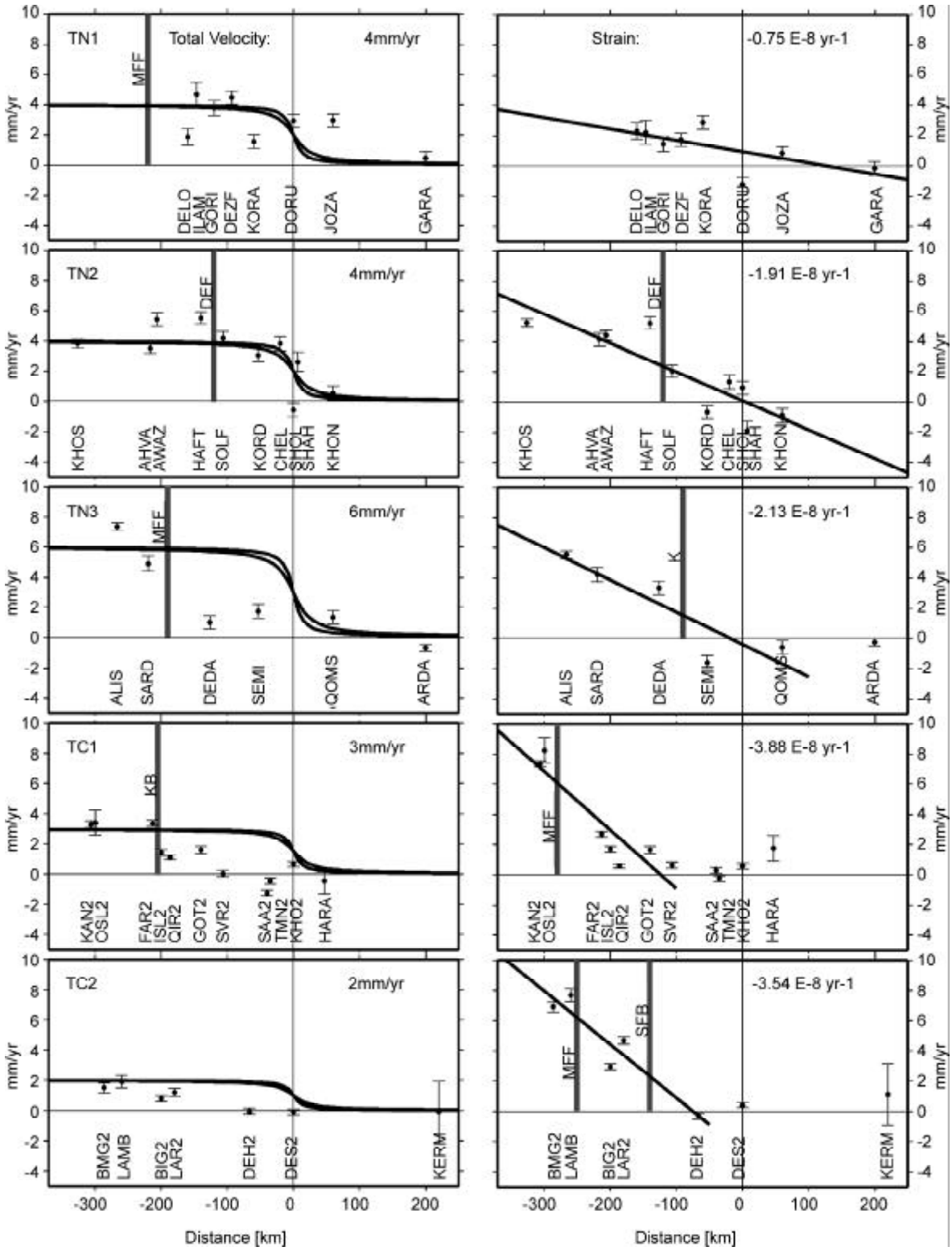

Figure 4. Site velocities (mm/yr) with respect to the site distance to the MRF/MZRF (in km, on the x axis) on 5 transects, TN1, TN2 and TN3 in the North Zagros, TC1 and TC2 in the Central Zagros, from northwest to southeast. On the left, we display the fault parallel components (strike-slip component) and on the right the fault perpendicular component (shortening). The site names are mentioned in order of the distance to the fault below the velocity vectors. A simple model is superposed on the individual velocities (dark grey line, for details see text). Light grey vertical lines indicate velocity discontinuities at active fault locations.

of Figure (4)) in Central Zagros (transect *TC*2), two sudden velocity increases are noted: between *DEH*2 and *LAR*2 when crossing the Simple Fold Belt, and between *BIG*2 and *LAMB* when crossing the Main Front Fault (*MFF*). On the *TN*3 transect, the strike-slip activity of the Kazerun fault can be recognized in the shortening component (between *SEMI* and *DEDA*) because of its oblique orientation (*NS*) with respect to *MRF/MZRF*. On the *TN*2 transect some evidence can be found for the activity of the Dezful Embayment fault (*DEF*), situated between the sites *KORD* and *SOLE*. In the strike-slip component (left part of Figure (4)) of the same transect, the *DEF* can be noticed as well.

Further to the east (*TN*3), this zone of deformation is represented by the Zagros Mountain Front fault (*ZMFF*), localized between *DEDA* and *SARD*. To the west of North Zagros (*TN*1), there is no site south of *ZMFF*, so it can be suspected that we miss another velocity increase on this transect. In the Central Zagros (*TC*1), the Kareh Bas fault can be identified as well as presently active feature according to the velocity increase between *FAR*2 and *ISL*2, in the zone of its emplacement.

This study gives some evidence for the activity of individual faults which can be focused on in dedicated studies. However, the precise evaluation of individual displacement rates on faults in North Zagros requires a third measurement campaign to be carried out and included in the analysis.

6. First Velocity Estimates of the Kazerun Fault System

Our present study can be used to extrapolate some first velocity estimates on different segments of the Kazerun fault system, by comparing the velocity fields in the North and the Central Zagros to each side of the fault system, see Figure (2). From south to north, 5*mm/yr* of relative *NS* displacement between *ALIS* and *FAR*2 is obtained, characterizing the slip rate on the Borazjan fault, 6*mm/yr* between *SARD* and the Central Iranian block, at the latitude of the Kazerun segment, and 3*mm/yr* between *DEDA* and the Central Iranian block which can be attributed to the Dena fault. These first far field velocity estimates confirm that the Kazerun fault system is a major tectonic feature in the Zagros kinematics.

7. Conclusions

Two measurement campaigns on the North Zagros *GPS* network have been sufficient to evaluate a coherent velocity field with differential velocities between 0 and 6*mm/yr*, thanks to the forced antenna centring.

The global North Zagros present day deformation can be characterized by 3-6*mm/yr* of shortening and 4-6*mm/yr* of right lateral strike-slip, coherent with first estimates from the larger scale Iran global *GPS* network [9] and indicating clearly lower strike-slip activity on the *MRF* than proposed by Talebian and Jackson [6].

This study was the opportunity to compare a first velocity estimate on the North Zagros network with the velocity field obtained in the Central Zagros based on 3 measurement campaigns. With respect to Central Zagros where 8*mm/yr* of shortening and 2-3*mm/yr* of strike-slip motion are observed, an increase of the global strike-slip rate and a decrease of the global shortening rate in North Zagros can be stated.

While the Central Zagros velocity field shows a relatively simple deformation pattern (stable northern part with respect to the Central Iranian block, shortening concentrated close to the Persian Gulf coastline, only a slight strike-slip component in the western part of the network), the North Zagros velocity field based on only two campaigns is relatively diffuse with decreasing velocities from the Persian Gulf plane to the Central Iranian block and the presence of shortening and strike-slip mechanisms. However, some places of concentrated deformation have been identified, which means that the North Zagros deformation is rather localized on individual faults (*DEF, ZMFF, MRF*) than distributed. Nevertheless, at the time being, there is no clear evidence for partitioning of the deformation mechanisms on spatially separated strike-slip and thrust faults. The global Zagros deformation pattern as deduced by the two networks has been characterized by one (narrow) zone of deformation in the southern part of Central Zagros which is transferred to two bands of significant deformation in North Zagros (one centred on the *DEF*, one centred on *MRF*). The transfer takes place at the localization of the Kazerun fault system which seems to play a major role in the global Zagros deformation mechanism.

Acknowledgements

The *GPS* campaigns presented here have been successful, thanks to the help of many colleagues: F. Masson and M. Peyret (*LDL* Montpellier), M.-N. Bouin (*LAREG* St. Mandé), C. Sue (Univ. Neuchâtel),

F. Nilforoushan (*NCC*), and the field teams of *NCC* and *IIEES*. This project was financed by the *CNRS-INSU* "Intérieur de la Terre" programme, the *NCC* and the *IIEES*. The GPS receivers were provided by *CNRS-INSU* and *NCC*.

References

1. Berberian, M. (1995). "Master Blind Thrust Faults Hidden under the Zagros Folds: Active Basement Tectonics and Surface Morphotectonics", *Tectonophysics*, **241**, 193-224.

2. DeMets, C., Gordon, R.G., Argus, D.F., and Stein, S. (1994). "Effects of Recent Revisions to the Geomagnetic Reversal Time Scale on Estimates of Current Plate Motions", *Geophys. Res. Lett.*, **21**, 2191-2194.

3. King, R.W. and Bock, Y. (2002). "Documentation for the GAMIT Analysis Software, Release 10.1", Massachusetts Institute of Technology, Cambridge, MA.

4. Savage, J. and Burford, R. (1973). "Geodetic Determination of Relative Plate Motion in Central California", *J. Geophys. Res.*, **95**, 4873-4879.

5. Sella, G.F., Dixon, T.H., and Mao, A. (2002). "REVEL: A Model for Recent Plate Velocities from Space Geodesy", *J. Geophys. Res.*, **107**(B4), ETG 11-1, 11-32.

6. Talebian, M. and Jackson, J. (2002). "Offset on the Main Recent Fault of the NW Iran and Implications on the Late Cenozoic Tectonics of the Arabia-Eurasia Collision Zone", *Geophys. J. Int.*, **150**, 422-439.

7. Talebian, M. and Jackson, J. (2004). "A Reappraisal of Earthquake Focal Mechanisms and Active Shortening in the Zagros Mountains of Iran", *Geophys. J. Int.*, **156**, 506-526.

8. Tatar, M., Hatzfeld, D., Martinod, J., Walpersdorf, A., Ghafory-Ashtiany, M., and Chéry, J. (2002). "The Present-Day Deformation of the Central Zagros from GPS Measurements", *Geophys. Res. Lett.*, **29**(19), 1927.

9. Vernant, P., Nilforoushan, F., Hatzfeld, D., Abbassi, M.R., Vigny, C., Masson, F., Nankali, H., Martinod, J., Ghafory-Ashtiany, M., Bayer, R., Tavakoli, F., and Chéry, J. (2004). "Present-Day Crustal Deformation and Plate Kinematics in the Middle East Constrained by GPS Measurements in Iran and Northern Oman", *Geophys. J., Int.*, **157**, 381-398.